Polymer 50 (2009) 2087–2094

Contents lists available at ScienceDirect

Polymer

journal homepage: www.elsevier.com/locate/polymer

Synthesis, morphology and mechanical properties of linear triblock copolymers based on poly(α-methylene-γ-butyrolactone)

Jaroslav Mosnáček [a,b], Jeong Ae Yoon [a], Azhar Juhari [c], Kaloian Koynov [c], Krzysztof Matyjaszewski [a,*]

[a] Department of Chemistry, Carnegie Mellon University, 4400 Fifth Avenue, Pittsburgh, PA 15213, USA
[b] Polymer Institute, Slovak Academy of Sciences, Dúbravská cesta 9, 842 36 Bratislava, Slovak Republic
[c] Max-Planck-Institute for Polymer Research, P.O. Box 3148, D-55021 Mainz, Germany

ARTICLE INFO

Article history:
Received 5 January 2009
Accepted 24 February 2009
Available online 3 March 2009

Keywords:
ATRP
Block copolymers
Thermoplastic elastomers

ABSTRACT

A series of well-defined triblock copolymers containing middle soft poly(*n*-butyl acrylate) (PBA) block and outer hard blocks of poly(α-methylene-γ-butyrolactone) homopolymer (PMBL) or random poly (α-methylene-γ-butyrolactone)-*r*-poly(methyl methacrylate) copolymer (PMBL-*r*-PMMA) were synthesized by atom transfer radical polymerization (ATRP). Phase separated morphologies of cylindrical or spherical hard block domains arranged in the soft PBA matrix were observed by atomic force microscopy and small-angle X-ray scattering. The mechanical and thermal properties of the copolymers were thoroughly characterized and their thermoplastic elastomer behavior was studied. Dynamic mechanical analysis (DMA) showed for all PMBL-*b*-PBA-*b*-PMBL copolymers a very broad rubbery plateau range extending up to temperatures of 300 °C. Replacement of the PMBL hard block with the less brittle PMBL-*r*-PMMA resulted in an improvement of the tensile properties, without compromising the very good thermal stability of the materials.

1. Introduction

Thermoplastic elastomers (TPEs) form an important class of materials combining elastomeric behavior with thermoplastic properties. Commonly these are ABA type triblock copolymers that combine a soft central block with glassy end blocks. These blocks should be immiscible and should phase separate with formation of thermoplastic microdomains, which act as physical cross-links for the soft matrix. One of the most common TPEs is the polystyrene–polybutadiene–polystyrene (SBS) triblock copolymer [1]. However, SBS suffers from two drawbacks. First, the unsaturated polybutadiene block is easily oxidized and is sensitive to UV degradation. Second, the upper service temperature is limited by T_g of the polystyrene block (ca. 100 °C). Therefore, there is a continuous effort to replace polystyrene by thermoplastics with higher T_g and also substitute polybutadiene with more stable rubbery blocks [2]. Various fully acrylic TPEs based on combination of polyacrylates as soft blocks with different polymethacrylates as hard blocks were synthesized by anionic [3,4] or controlled radical polymerization [5–10] techniques. The versatile (meth)acrylic monomers cover a wide range of T_g from ca. −50 to +200 °C. Furthermore, these polymers are not sensitive to UV and oxidation.

Recently, we reported the preparation of well-defined homopolymers as well as diblock and triblock copolymers of α-methylene-γ-butyrolactone (MBL) using atom transfer radical polymerization (ATRP) [11]. MBL, found in tulips, is the simplest member of butyrolactones found and isolated from various plants [12–15]. Such natural products are renewable, environmentally friendly, biocompatible, and biodegradable. Also, they may possess some special physical and biomedical properties. Recently a possibility of using natural products to replace petroleum-based raw materials in large commodity markets, such as plastics, fibers, and fuels has been reviewed [16,17]. MBL consists of a five-membered ring with an ester group and possesses structural features similar to those of methyl methacrylate and polymerizes in a similar manner. Poly(α-methylene-γ-butyrolactone) (PMBL) has good durability, a high refractive index (1.540) [18], and high T_g (195 °C) [19]. Various copolymers and blends containing MBL units have good optical properties and resistance to heat, weathering, scratches and solvents [20].

The physical properties of PMBL, such as high T_g and limited solubility, could be beneficial for its use as hard component in thermoplastic elastomers. Therefore, the linear triblock copolymers with soft PBA control segments were prepared (see Scheme 1) and their morphology and mechanical properties were investigated.

* Corresponding author. Tel.: +1 412 268 3209; fax: +1 412 268 6897.
E-mail address: km3b@andrew.cmu.edu (K. Matyjaszewski).

0032-3861/$ – see front matter © 2009 Elsevier Ltd. All rights reserved.
doi:10.1016/j.polymer.2009.02.037

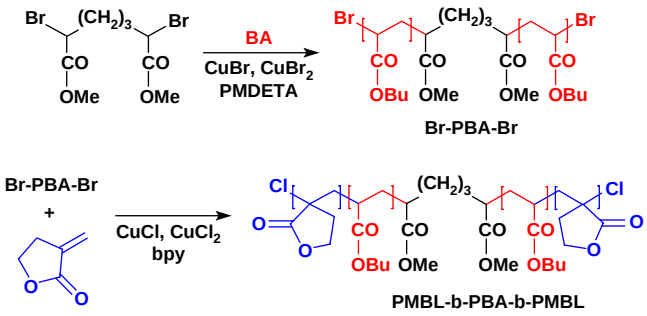

Scheme 1. Preparation of PMBL-*b*-PBA-*b*-PMBL triblock copolymers.

2. Experimental section

2.1. Materials

α-Methylene-γ-butyrolactone (MBL), *n*-butyl acrylate (BA), and methyl methacrylate (MMA) were purchased from Aldrich and purified by passing it through an alumina column to remove stabilizers. DMF, anisole, and methanol (all from Aldrich) were used as-received. CuBr and CuCl were purified according to the literature procedures [21]. $CuBr_2$, $CuCl_2$, ligands 2,2′-bipyridine (bpy) [22] and *N*,*N*,*N*′,*N*′,*N*″-pentamethyldiethylenetriamine (PMDETA) [23], and initiators 2-bromopropionitrile (BPN) [24] and dimethyl 2,6-dibromoheptanedionate (DMDBH) [25] (all from Aldrich) were used as-received.

2.2. Synthesis of difunctional poly(n-butyl acrylate) macroinitiator (Br–PBA–Br)

Difunctional Br–PBA–Br macroinitiator with the molecular weight $M_n = 27\,500$ g/mol and the distribution of molecular weights $M_w/M_n = 1.07$ was prepared as follows: a round bottomed flask containing *n*-butyl acrylate, dimethyl 2,6-dibromoheptanedionate, *N*,*N*,*N*′,*N*′,*N*″-pentamethyldiethylenetriamine (PMDETA), and anisole (20 wt%) was degassed by three freeze–pump–thaw cycles. Then, CuBr was added to the frozen reaction solution under nitrogen flow. The flask was closed, evacuated, back-filled with nitrogen, and immersed in an oil bath thermostated at 80 °C. Ratio of monomer:initiator:CuBr:ligand 400:1:0.8:0.8 was used and the polymerization was stopped at 53% of the monomer conversion. Br–PBA–Br macroinitiator was purified by passing through an activated neutral alumina column followed by the removal of the solvent and the unreacted monomer by evaporation and air flowing.

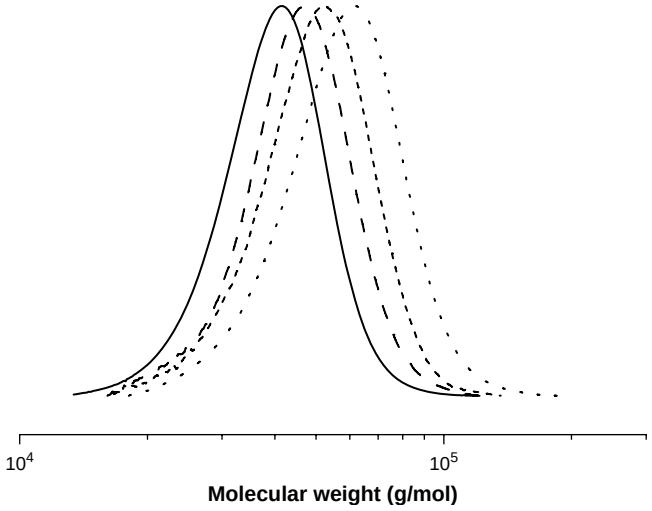

Fig. 1. GPC traces of PMBL-*b*-PBA-*b*-PMBL triblock copolymers prepared by chain extension from (—) Br–PBA–Br macroinitiator ($M_n = 48\,200$ g/mol; $M_w/M_n = 1.08$); (– –) BA375-MBL32 ($M_n = 51\,300$ g/mol; $M_w/M_n = 1.09$); (– – –) BA375-MBL60 ($M_n = 54\,100$ g/mol; $M_w/M_n = 1.10$); (···) BA375-MBL144 ($M_n = 62\,400$ g/mol; $M_w/M_n = 1.12$).

Difunctional poly(*n*-butyl acrylate) macroinitiator (Br–PBA–Br) with the molecular weight $M_n = 48\,200$ g/mol and distribution of molecular weights $M_w/M_n = 1.08$ was provided by ATRP Solutions Inc.

2.3. Synthesis of triblock copolymers

The general procedure for the chain extension of the Br–PBA–Br macroinitiator was as follows: a round bottomed flask containing MBL or MMA or a mixture of MBL and MMA, Br–PBA–Br macroinitiator, $CuCl_2$, 2,2′-bipyridine, and DMF was degassed by three freeze–pump–thaw cycles. Then, CuCl was added to the frozen reaction solution under nitrogen flow. The flask was closed, evacuated, back-filled with nitrogen, and immersed in an oil bath thermostated at 50 °C. Ratio of monomer:initiator:CuCl:$CuCl_2$:ligand was used as described in Table 1.

2.4. General analysis

Monomer conversions and molecular weights of final triblock copolymers were determined by ^{1}H NMR on a 300 MHz Bruker NMR spectrometer using DMF-d_7 as a solvent. Molecular weights as well as molecular weight distributions of the macroinitiator and

Table 1
Experimental conditions of ATRP of MBL and characterization of prepared polymers.

Entry	M1	M2	I	CuCl	$CuCl_2$	L	DMF	Time	Conv.[c]	$M_{n,\,theor}$	$M_{n,\,exp.}$[c]	M_w/M_n[d]
1	75	–	1[a]	2.2	0.2	2.4	45 vol%	4 h	45%	30 810	31 800	1.09
2	75	–	1[a]	2.2	0.2	2.4	45 vol%	15 h	95%	34 490	34 600	1.11
3	125	–	1[a]	2.2	0.2	2.4	55 vol%	11 h	91%	38 660	39 500	1.11
4	100	–	1[b]	2.2	0.2	4.8	50 vol%	5.5 h	36%	51 730	51 300	1.09
5	195	–	1[b]	2.2	0.2	2.4	45 vol%	7 h	33%	54 510	54 100	1.10
6	195	–	1[b]	2.2	0.2	2.4	45 vol%	22 h	65%	60 630	62 400	1.12
7	142.5	47.5	1[b]	2.2	0.2	4.8	43 vol%	20 h	64%	60 780	61 200	1.11
8	95	95	1[b]	2.2	0.2	4.8	43 vol%	19 h	61%	59 770	61 200	1.12
9	–	220	1[b]	2.2	0.2	4.8	40 vol%	19.5 h	60%	61 420	61 400	1.10

M1, M2, I, and L stand for α-methylene-γ-butyrolactone, methyl methacrylate, Br–PBA–Br macroinitiator and 2,2′-bipyridine, respectively.
[a] Br–PBA–Br macroinitiator with $M_n = 27\,500$ g/mol, $M_w/M_n = 1.07$ based on GPC using PS standards.
[b] Br–PBA–Br macroinitiator with $M_n = 48\,200$ g/mol, $M_w/M_n = 1.08$ based on GPC using PS standards.
[c] Based on ^{1}H NMR spectra.
[d] Based on GPC using PS standards.

Table 2
Composition of prepared triblock copolymers.

Entry	Label	Triblock composition	Hard block (mol%)[a]	Hard block (wt%)[a]	MBL/MMA (mol%)[a]
1	BA215-MBL40	$PBA_{215}(-b\text{-}PMBL_{20})_2$	15.8	12.6	100/0
2	BA215-MBL68	$PBA_{215}(-b\text{-}PMBL_{34})_2$	23.7	19.3	100/0
3	BA215-MBL120	$PBA_{215}(-b\text{-}PMBL_{60})_2$	36.3	30.3	100/0
4	BA375-MBL32	$PBA_{375}(-b\text{-}PMBL_{16})_2$	7.9	6.1	100/0
5	BA375-MBL60	$PBA_{375}(-b\text{-}PMBL_{30})_2$	13.8	10.9	100/0
6	BA375-MBL144	$PBA_{375}(-b\text{-}PMBL_{72})_2$	27.6	22.7	100/0
7	BA375-MBL106MMA26	$PBA_{375}(-b\text{-}PMBL_{53}\text{-}r\text{-}PMMA_{13})_2$	26.0	21.3	80/20
8	BA375-MBL82MMA50	$PBA_{375}(-b\text{-}PMBL_{41}\text{-}r\text{-}PMMA_{25})_2$	26.0	21.4	62/38
9	BA375-MMA132	$PBA_{375}(-b\text{-}PMMA_{66})_2$	26.0	21.6	0/100

[a] Based on ^{1}H NMR spectra.

triblock copolymers were measured using GPC (Polymer Standards Services (PSS) columns (guard, 10^5, 10^3, and 10^2 Å) with DMF (containing 5 mM LiBr) as an eluent at 50 °C, flow rate 1.00 mL/min, and differential refractive index (RI) detector (Waters, 2410)). Toluene was used as the internal standard to correct for any fluctuation in DMF flow rate. The apparent molecular weight and the molecular weight distribution were determined with a calibration curve based on linear polystyrene standards.

2.5. Tapping mode atomic force microscopy (TMAFM)

The polymers dissolved in DMF (1 mg/mL) were deposited by drop casting onto silicon wafer surface (0.7 cm × 0.7 cm) cleaned by rinsing with acetone and isopropanol followed by oxygen plasma treatment. The samples were dried under house vacuum at room temperature for 8 h at least. Tapping mode AFM experiments were carried out using a Multimode Nanoscope III system (Digital Instruments, Santa Barbara, CA). The measurements were performed in air using commercial Si cantilevers with a nominal spring constant and resonance frequency of 5 N/m and 130 kHz respectively. The height and phase images were acquired simultaneously at set-point ratio $A/A_0 = 0.8$–0.9, where A and A_0 refer, respectively, to the "tapping" and "free" cantilever amplitude. Annealing of the samples was performed in an oven under nitrogen at 210 °C for 30 min. After annealing, the oven was turned off and the cooling occurred naturally. The AFM images from the annealed samples were taken under the same conditions as mentioned above.

2.6. Power spectral analysis of TMAFM images

Phase AFM images showing enough contrast periodicities were analyzed by a 2-D Fourier transform (FT). Subsequently, the 2-D FT maps were azimuthally averaged to produce magnitude plots analogous to the scattering patterns. After recalculating the spatial frequency scale to scattering vector units (q, $2\pi/d$), the domain spacing (d) was calculated from the q value that showed the peak maximum of the power spectrum.

2.7. Small-angle X-ray scattering analysis (SAXS)

SAXS measurements were conducted using a rotating anode (Rigaku RA-Micro 7) X-ray beam with a pinhole collimation and a two-dimensional detector (Bruker Highstar) with 1024 × 1024 pixels. A double graphite monochromator for the Cu Kα radiation ($\lambda = 0.154$ nm) was used. The beam diameter was about 0.8 mm, and the sample to detector distance was 1.8 m. The recorded scattered intensity distributions were integrated over the azimuthal angle and are presented as functions of the scattering vector ($s = 2\sin(\theta)/\lambda$, where 2θ is the scattering angle).

2.8. Dynamic mechanical analysis (DMA)

DMA was performed on a Rheometrics RMS 800 mechanical spectrometer. Shear deformation was applied under conditions of controlled deformation amplitude, which was kept in the range of the linear viscoelastic response of studied samples. Plate–plate geometry was used with plate diameters of 6 mm. Experiments have been performed under a dry nitrogen atmosphere. Results are presented as temperature dependencies of the storage (G') and loss (G'') shear moduli measured at a constant deformation frequency of 10 rad/s. The results were obtained with a 2 °C/min heating rate.

2.9. Tensile tests

Tensile tests were performed using a mechanical testing machine Instron 6000. Samples with thickness in the order of 0.2–0.5 mm were drawn with the rate of 5 mm/min at room or at elevated temperature. Dependencies of stress vs. draw ratio were recorded. Elastic modulus, elongation at break and stress at break were determined by averaging of 3–5 independent drawing experiments performed at the same conditions.

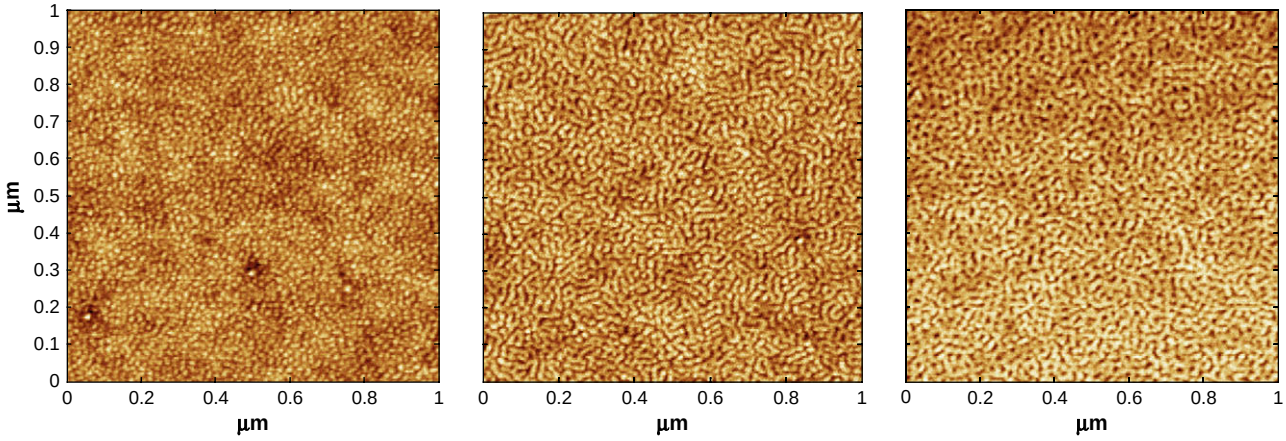

Fig. 2. AFM phase images of PMBL–PBA–PMBL triblock copolymers: (left) BA215-MBL40 (12.6 wt% PMBL); (middle) BA215-MBL68 (19.3 wt% PMBL); and (right) BA215-MBL120 (30.3 wt% PMBL).

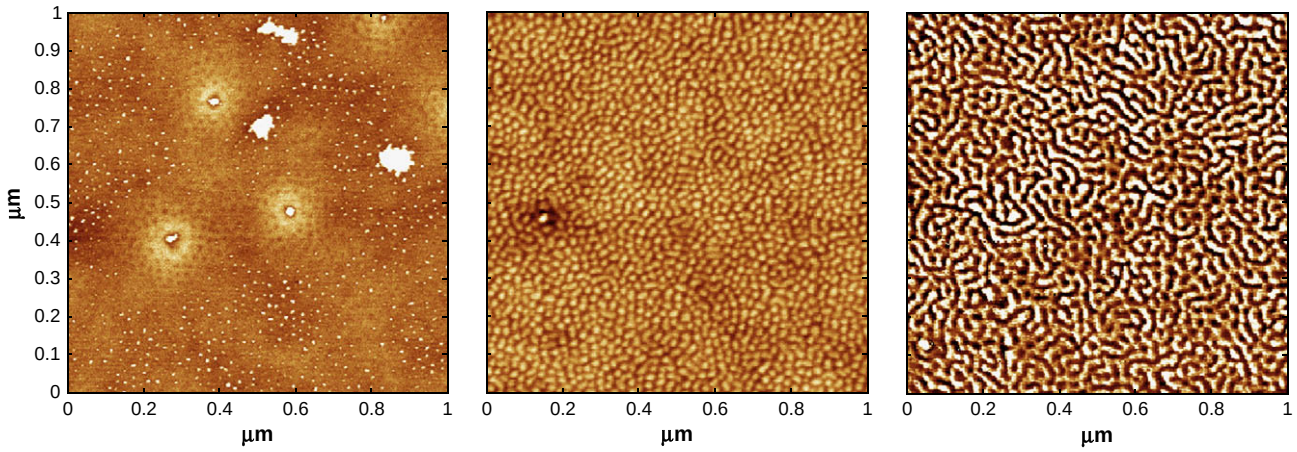

Fig. 3. AFM phase images of PMBL–PBA–PMBL triblock copolymers: (left) BA375-MBL32 (6.1 wt% PMBL); (middle) BA375-MBL60 (10.9 wt% PMBL); and (right) BA375-MBL144 (22.7 wt% PMBL).

3. Results and discussion

3.1. Synthesis

As the ATRP equilibrium constants for MBL and MMA are much higher than that for BA, chain extension of PBA macroinitiator involved the halogen exchange strategy to provide for higher, or at least equal, rate of crosspropagation, in comparison with rate of propagation [26,27]. Experimental conditions for preparation of all studied copolymers are given in Table 1. Feed ratios of MBL:MMA in the Entries 7 and 8 were 75:25 and 50:50, respectively. Final ratios of comonomers in the resulting copolymers were 80:20 and 62:38 for Entries 7 and 8, respectively, in agreement with reactivity ratios $r_{MBL} = 1.67$ and $r_{MMA} = 0.6$ reported for a free radical copolymerization of MBL and MMA [28].

An example of evolution of GPC traces with conversion for block extension from PBA macroinitiator with DP = 375 ($M_n = 48\,200$ g/mol) with MBL segments is shown in Fig. 1. A smooth shift of the molecular weight was observed. All copolymers had low polydispersities, as reported in Table 1. The compositions of the prepared triblock copolymers were determined by ^{1}H NMR and are given in Table 2.

3.2. Morphology of the PMBL–PBA–PMBL copolymers

Because of the incompatibility between PBA and PMBL, the prepared triblock copolymers were expected to show strong phase separation. In order to visualize this effect, an AFM imaging on thin films prepared by drop casting of the polymer solutions in DMF onto silicon wafer substrates was performed for all prepared copolymers. Typical results are shown in Figs. 2 and 3 revealing a phase separated morphology of rigid PMBL domains (brighter features in the AFM images) dispersed in the softer PBA matrix. The copolymers BA215-MBL68, BA215-MBL120, and BA375-MBL144 with PMBL content higher than 19 wt% showed elongated features originating from PMBL cylinders preferentially oriented parallel to the film surface (see Figs. 2 and 3). On the other hand, the copolymers BA215-MBL40 and BA375-MBL60 containing 12.6 and 10.9 wt% of PMBL, respectively, showed more randomly oriented cylindrical morphologies (see Figs. 2 and 3). The copolymer BA375-MBL32 with PMBL content of only 6.1 wt% showed spherical morphology and some aggregates of hard PMBL blocks (see Fig. 3).

Some of the prepared samples were annealed at 210 °C (above the T_g of PMBL block) and the morphology after annealing was investigated. Nitrogen atmosphere was applied during the

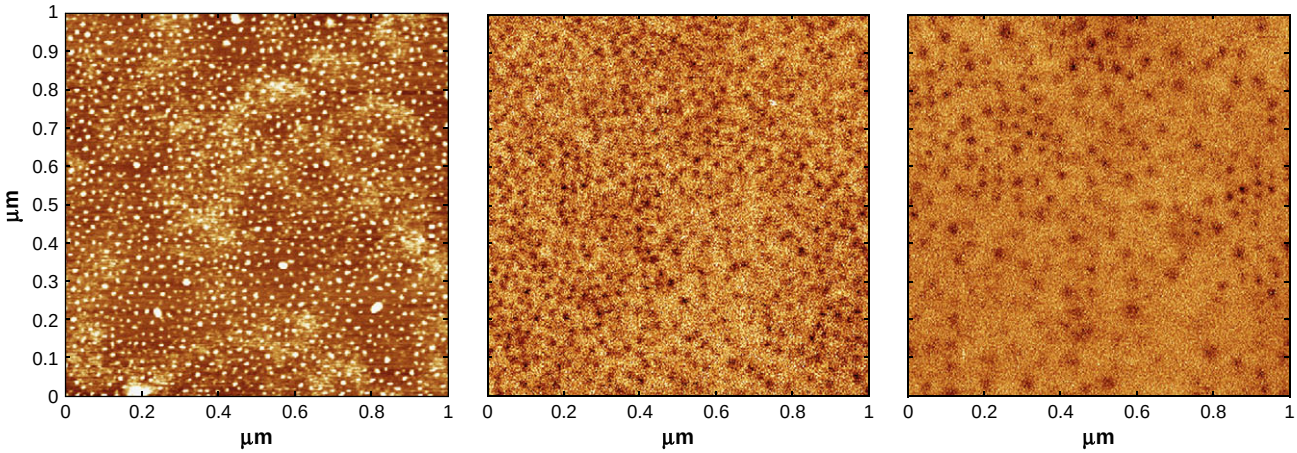

Fig. 4. AFM phase images of PMBL–PBA–PMBL triblock copolymers after annealing for 30 min at 210 °C under nitrogen atmosphere: (left) BA375-MBL32 (6.1 wt% PMBL); (middle) BA375-MBL60 (10.9 wt% PMBL); and (right) BA3755-MBL144 (22.7 wt% PMBL).

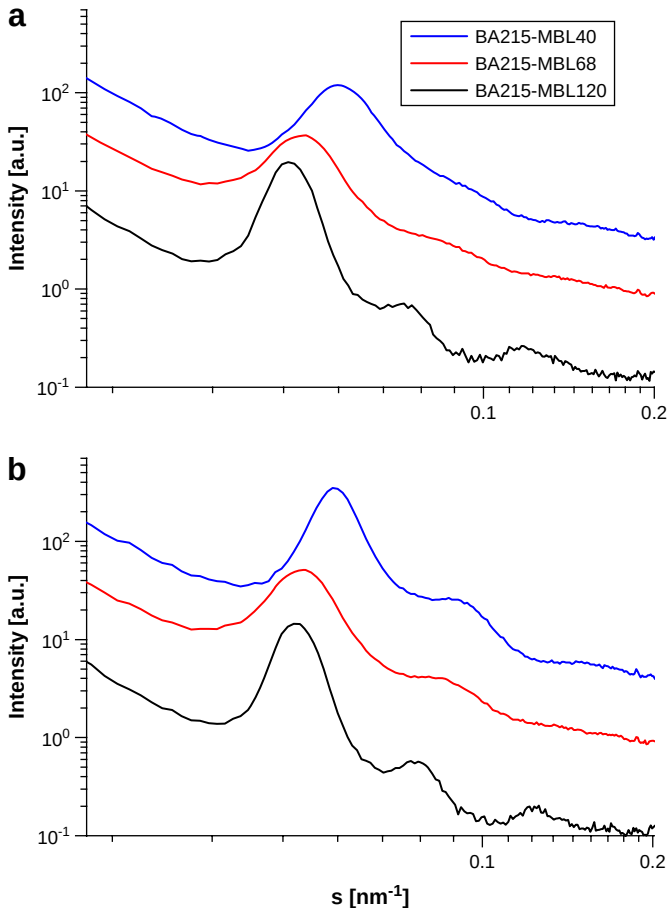

Fig. 5. SAXS spectra of PMBL–PBA–PMBL triblock copolymers with constant PBA segments length and increasing PMBL length (a) before and (b) after annealing for 30 min at 150 °C under nitrogen atmosphere.

annealing in order to prevent oxidation of the polymers. After 30 min of annealing, the AMF images still showed phase separation, although morphology changes were observed (see Fig. 4). In the case of BA375-MBL32 with spherical morphology, the AFM image showed partial destruction of aggregates and more regular distribution of spheres. Moreover, spacing between spheres, calculated

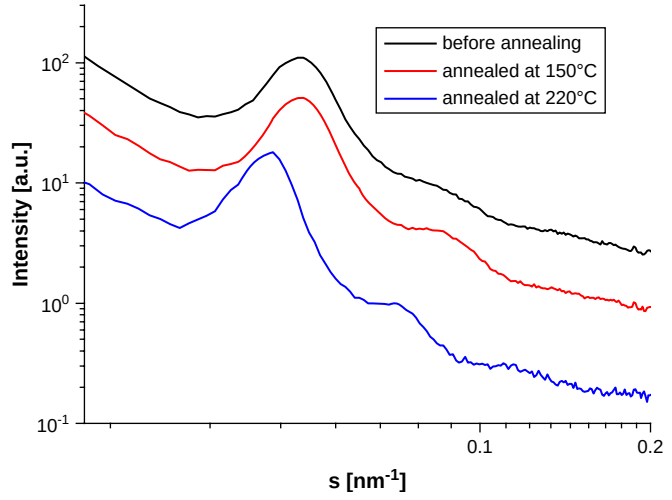

Fig. 6. SAXS spectra of the BA215-MBL68 before and after annealing at different temperatures.

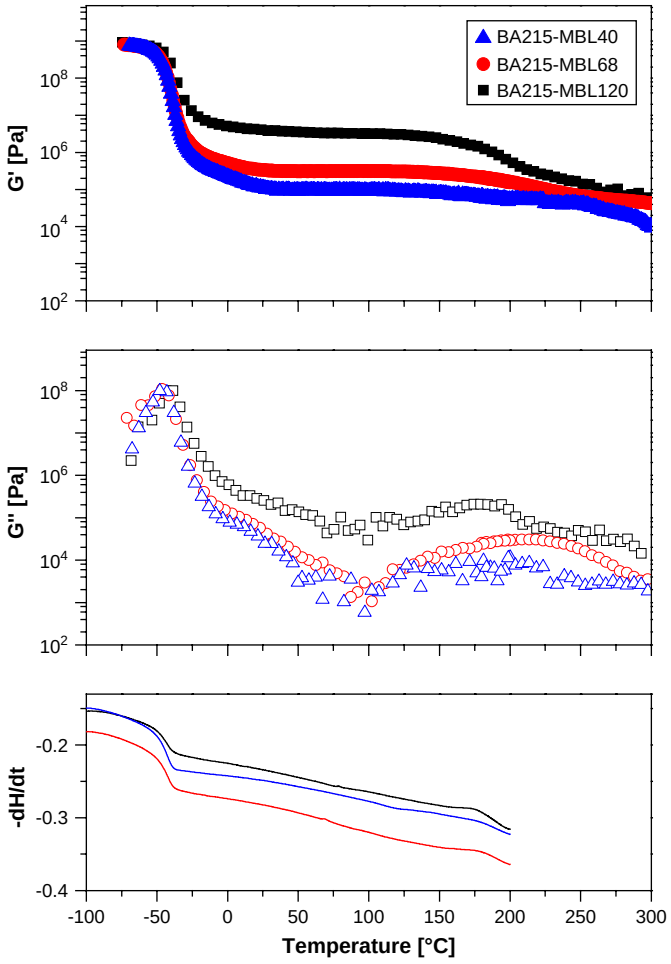

Fig. 7. Thermo-mechanical (2 °C/min) and DSC (10 °C/min) analysis of PMBL–PBA–PMBL triblock copolymers.

from AFM images, changed from 24 nm to 28 nm by annealing. Change in morphology was observed also after annealing of BA375-MBL60 copolymer. The randomly oriented cylinders were reoriented by annealing to give cylinders oriented perpendicular to the surface. At the same time, the spacing between the cylinders, calculated from AFM images, changed from 26 nm to 30 nm by annealing. Similarly, in the case of BA375-MBL144 copolymer, annealing changed the parallel orientation of cylinders to the perpendicular to the surface. At the same time, the domain spacing became less regular and it was difficult to obtain a sharp peak from the power spectrum of the AFM image and determine a spacing value. The spacing between the cylinders before annealing, calculated from the AFM images, was 31.5 nm.

SAXS analysis of thick films of the PMBL–PBA–PMBL triblock copolymers was performed in order to get a better insight on the effect of phase separation and the resulting microstructures. Typical results are presented in Fig. 5. Samples which did not undergo any additional thermal treatment were studied first. As shown in Fig. 5a, only the copolymer with a high PMBL content (BA215-MBL120, 30.3 wt% PMBL) showed a well-ordered structure, consistent with hexagonally packed cylinders (three relatively sharp peaks at relative positions s, $\sqrt{3}s$, $\sqrt{7}s$). The samples with moderate PMBL content (19.3 and 12.6 wt% PMBL) did not exhibit well defined secondary peaks, indicating mainly short-range ordered. The SAXS experiments were then repeated after thermal annealing of the PMBL–PBA–PMBL samples at 150 °C for 1 h in

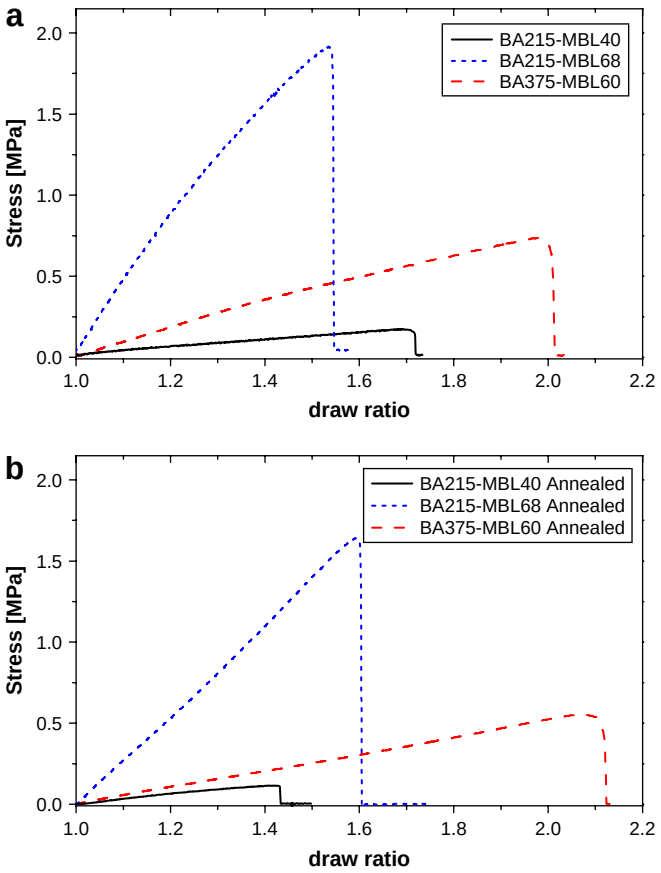

Fig. 8. Tensile mechanical properties of PMBL–PBA–PMBL triblock copolymers with different compositions: (a) before and (b) after thermal annealing at 150 °C for 1 h.

order to examine the effect of the annealing process on the morphology of the copolymer films. The comparison of Fig. 5b with Fig. 5a shows that the annealed films exhibited better ordering than the untreated samples, displaying at least three scattering peaks in each of the SAXS spectra. Furthermore, the ratios of the relative peak positions in all cases were s, $\sqrt{3}s$, $\sqrt{7}s$, i.e. consistent with a hexagonal lattice. A closer look at Fig. 5 shows that for the same length of the PBA segment, an increase in PMBL block length leads to increase in the d-spacing. Similar cylindrical morphology was observed via SAXS for most PMBL–PBA–PMBL copolymers.

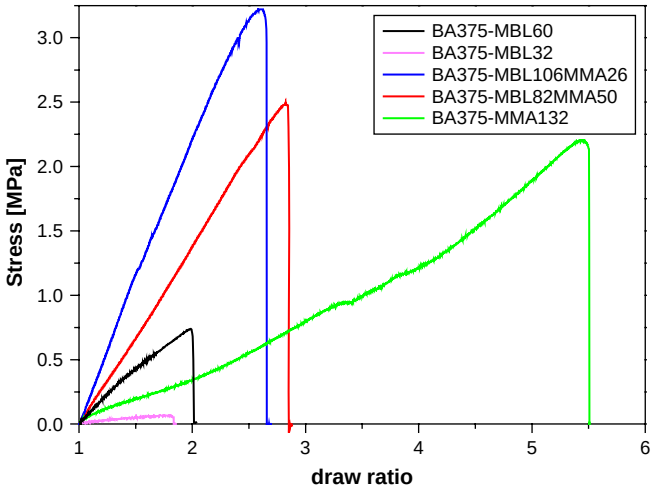

Fig. 10. Tensile mechanical properties of (PMBL-*r*-PMMA)-PBA-(PMBL-*r*-PMMA) triblock copolymers compared to that of PMBL–PBA–PMBL.

The AFM studies showed that PMBL–PBA–PMBL copolymers retain their phase separated morphology even when annealed at temperatures above the T_g of the hard PMBL component. This finding was further confirmed by SAXS experiments. Fig. 6 compares the SAXS spectra of as prepared thick films of BA215-MBL68 with those measured after annealing at 150 °C and 220 °C, respectively. The hexagonal morphology remained phase separated even after heating the copolymers to temperatures above the softening temperature of PMBL.

3.3. Thermo-mechanical properties of PMBL–PBA–PMBL copolymers

Dynamic mechanical properties of the PMBL–PBA–PMBL linear triblock copolymers were characterized through the temperature dependencies of the real (G') and the imaginary (G'') parts of the complex shear modulus. Typical results for series of copolymers with constant PBA content (DP = 215) and varying PMBL block lengths are shown in Fig. 7 together with the respective DSC thermographs. Two distinct glass transition temperatures corresponding to the PBA ($T_g \sim -50$ °C) and PMBL ($T_g \sim 195$ °C) segments, respectively, were observed in both DMA and DSC data. This provides an additional evidence for the microphase separated

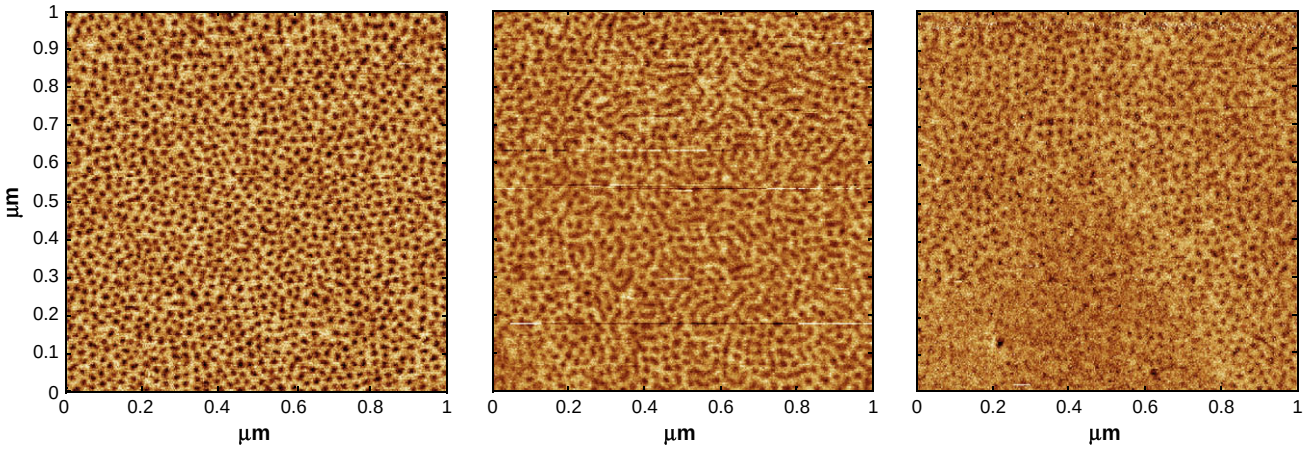

Fig. 9. AFM phase images of BA375-MMA132 copolymer: (left) before annealing; and (middle and right) after annealing for 30 min at 210 °C under nitrogen atmosphere.

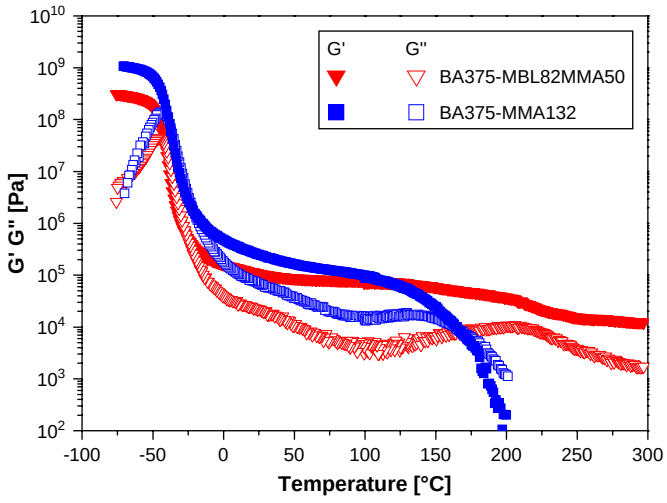

Fig. 11. Comparison of the thermo-mechanical properties of (PMBL-*r*-PMMA)–PBA–(PMBL-*r*-PMMA) and PMMA–PBA–PMMA triblock copolymers.

morphology of the copolymers. However, the glass transition of PMBL becomes less obvious with decreasing PMBL content. With respect to the mechanical properties, all samples were glassy below the glass transition temperature of PBA, with storage modulus $G' \approx 1$ GPa. Above this glass transition, the copolymers become elastic and show a G' plateau extending up to the softening temperature of PMBL ($\sim$195 °C). The height of the plateau strongly depends on the PMBL content. For example, the value of G' is ca. 0.1 MPa for PMBL fraction around 12 wt% and up to ca. 10 MPa for PMBL content of 30 wt%. In this elastic state the PMBL blocks form glassy domains connecting the flexible PBA blocks. This is a typical situation for a thermoplastic elastomer in which the hard phase elements or glassy domains act as physical cross-links for the flexible component.

The deep minimum of G'' observed in this rubbery plateau region is related to the very big difference in the glass transition temperatures of the soft and hard components. The data for G'' in the minimum are rather noisy due to profound elasticity of the copolymer, i.e. $G' >> G''$ that results in a very small phase angle $\tan\delta = G''/G'$, that approaches the resolution limit of the rheometer. Finally, both storage and loss moduli decreased above the T_g of PMBL but the copolymer did not flow in the studied temperature range of up to 300 °C.

The tensile mechanical properties of the PMBL–PBA–PMBL linear triblock copolymers were investigated and typical results are shown in Fig. 8a. The materials showed elastic behavior largely influenced by their composition. An increase of the hard component (PMBL) content resulted in a significant increase of elastic modulus and ultimate tensile strength. The elongation at break, however, was relatively low i.e. up to 100% and not clearly related to copolymer composition. Annealing the samples for 1 h at 150 °C did not help to improve the copolymer tensile properties, and elongation at break remained relatively low (see Fig. 8b). This effect is most likely related to the brittleness of the hard PMBL blocks [18,20,29].

In order to improve the tensile properties of the PMBL based copolymers, a series of ABA type triblock copolymers were prepared in which the outer hard blocks were replaced with a random copolymer of PMBL and PMMA. The morphology of these triblock copolymers (BA375-MBL106MMA26, BA375-MBL82MMA50), before as well as after annealing, was similar to described above morphology of BA375-MBL144 that has a similar hard block content. For comparison, a copolymer BA375-MMA132 containing only PMMA as a hard block was also prepared and studied. In thin films of this copolymer we found a regularly oriented cylindrical morphology perpendicular to the surface, that changed to cylinders oriented preferable parallel to the surface (see Fig. 9) after annealing. Moreover, AFM image could indicate also partial loss of separation for this material (see Fig. 9, right picture).

The (PMBL-*r*-PMMA)–PBA–(PMBL-*r*-PMMA) triblock copolymers exhibit better tensile properties than their PMBL–PBA–PMBL counterparts. As shown in Fig. 10, both elongation at break and ultimate tensile strength significantly increased up to values of $\sim$200% and $\sim$3.2 MPa, respectively. Nevertheless, the values of elongation at break are still significantly lower than those of the pure PMMA–PBA–PMMA triblock copolymer, of which stress–strain curve is also shown in Fig. 10.

Some limitations in the tensile properties of the PMBL–PBA–PMBL triblock copolymers may be related to incomplete chain extension, too short PMBL block, or the intrinsic brittleness of the PMBL.

While the tensile properties of the PMBL–PBA–PMBL and the (PMBL-*r*-PMMA)–PBA–(PMBL-*r*-PMMA) triblock copolymers are inferior to those of the PMMA–PBA–PMMA copolymer, they have significantly better thermal stability and retain their elastic properties up to very high working temperature of higher than 200 °C. This is illustrated in Fig. 11 that compares the temperature dependence of the shear moduli of BA375-MBL82MMA50 and BA375-MMA132. Both materials have similar molecular weights and hard block content. The copolymer with pure PMMA hard blocks shows a rubbery plateau that extends only to $\sim$120 °C. Furthermore, this material flowed at temperatures above 150 °C. In contrast, the rubbery plateau of BA375-MBL82MMA50 extends to more than 200 °C and no flow was observed up to 300 °C. The same is true also for the copolymers having pure PMBL hard blocks, as illustrated in Fig. 7. This effect is related to the very high glass transition temperature and high thermal stability [29] of PMBL that could make the PMBL based thermoplastic elastomers particularly suitable for high temperature applications.

4. Conclusions

In summary, linear PMBL–PBA–PMBL triblock copolymers with low polydispersities and with different molecular weights and compositions were synthesized by ATRP with the aid of halogen exchange. Solution cast films of the copolymers were studied by AFM and SAXS. Both methods revealed a microphase separated morphology of cylindrical PMBL domains hexagonally arranged in the PBA matrix. Only at the very low PMBL content (6.1 wt%), the spherical morphology was observed. The thermo-mechanical properties of these new materials were thoroughly characterized using a variety of techniques. The DMA studies confirmed the phase separated morphology of the copolymers, revealing a very broad elastic plateau in the storage shear modulus that extends over $\sim$250 °C between the glass transition temperatures of the two blocks. The linear PMBL–PBA–PMBL triblock copolymers showed a relatively low elongation at break that was increased by replacing the PMBL hard blocks with the less brittle PMBL-*r*-PMMA blocks. Due to the very high glass transition temperature and high thermal stability of PMBL, these materials could be suitable for high temperature applications. This illustrates possibility of expansion of the range of block copolymers accessible by ATRP [30–43].

References

[1] Holden G, Legge NR. Thermoplastic elastomers. In: Holden G, Legge NR, Quirk RP, Schroeder HE, editors. Munich, Germany: Hanser; 1996. p. 71.
[2] Morton M. Thermoplastic elastomers. In: Holden G, Schroeder HE, editors. Munich, Germany: Hanser; 1987. p. 67.
[3] Jerome R, Bayard P, Fayt R, Jacobs C, Varshney S, Teyssie P. Thermoplastic elastomers. In: Holden G, Legge NR, Quirk RP, Schroeder HE, editors. Munich, Germany: Hanser; 1996. p. 521.
[4] Tong JD, Leclere P, Doneux C, Bredas JL, Lazzaroni R, Jerome R. Polymer 2000;41:4617–24.
[5] Matyjaszewski K, Shipp DA, McMurtry GP, Gaynor SG, Pakula T. J Polym Sci Part A Polym Chem 2000;38:2023–31.
[6] Moineau C, Minet M, Teyssie P, Jerome R. Macromolecules 1999;32:8277–82.
[7] Matyjaszewski K, Spanswick J. Thermoplastic elastomers by controlled/living radical polymerization. In: Holden G, Kricheldorf HR, Quirk RP, editors. Thermoplastic elastomers. Munich, Germany: Hanser; 2004. p. 365.
[8] Braunecker WA, Matyjaszewski K. Prog Polym Sci 2007;32:93–146.
[9] Dufour B, Tang CB, Koynov K, Zhang Y, Pakula T, Matyjaszewski K. Macromolecules 2008;41:2451–8.
[10] Dufour B, Koynov K, Pakula T, Matyjaszewski K. Macromol Chem Phys 2008;209:1686–93.
[11] Mosnacek J, Matyjaszewski K. Macromolecules 2008;41:5509–11.
[12] van Rossum M, Alberda M, van der Plas LHW. Phytochemistry 1998;49:723–9.
[13] Wong HF, Brown GD. Phytochemistry 2002;59:99–104.
[14] Vuckovic I, Vujisic L, Vajs V, Tesevic V, Janackovic P, Milosavljevic S. J Serb Chem Soc 2006;71:127–33.
[15] Trendafilova A, Todorova M, Mikhova B, Vitkova A, Duddeck H. Phytochemistry 2006;67:764–70.
[16] Williams CK, Hillmyer MA. Polym Rev 2008;48:1–10.
[17] Meier MAR, Metzger JO, Schubert US. Chem Soc Rev 2007;36:1788–802.
[18] Brandenburg CJ. US6841627B2; 2005.
[19] Akkapeddi MK. Macromolecules 1979;12:546–51.
[20] Pickett JE and Ye Q. US2007/0122625; 2007.
[21] Keller RN, Wycoff HD. Inorg Syn 1946;2:1–4.
[22] Wang J-S, Matyjaszewski K. J Am Chem Soc 1995;117:5614–5.
[23] Xia JH, Matyjaszewski K. Macromolecules 1997;30:7697–700.
[24] Matyjaszewski K, Jo SM, Paik HJ, Shipp DA. Macromolecules 1999;32:6431–8.
[25] Jakubowski W, Matyjaszewski K. Macromolecules 2005;38:4139–46.
[26] Matyjaszewski K, Shipp DA, Wang J-L, Grimaud T, Patten TE. Macromolecules 1998;31:6836–40.
[27] Matyjaszewski K, Xia J. Chem Rev 2001;101:2921–90.
[28] Akkapeddi MK. Polymer 1979;20:1215–6.
[29] Schwind H, Hauch D, Hasskerl T, Dorn K, Hopp M. US5880235; 1999.
[30] Tsarevsky NV, Matyjaszewski K. Chem Rev 2007;107:2270.
[31] Gaynor SG, Matyjaszewski K. Macromolecules 1997;30:4241.
[32] Coca S, Paik HJ, Matyjaszewski K. Macromolecules 1997;30:6513.
[33] Matyjaszewski K, Beers KL, Kern A, Gaynor SG. J Polym Sci Part A Polym Chem 1998;36:823.
[34] Teodorescu M, Matyjaszewski K. Macromol Rapid Commun 2000;21:190.
[35] Shinoda H, Miller PJ, Matyjaszewski K. Macromolecules 2001;34:3186.
[36] Shinoda H, Matyjaszewski K. Macromolecules 2001;34:6243.
[37] Jakubowski W, Matyjaszewski K. Ang Chem-Int Ed 2006;45:4482.
[38] Matyjaszewski K, Dong HC, Jakubowski W, Pietrasik J, Kusumo A. Langmuir 2007;23:4528.
[39] Pietrasik J, Dong HC, Matyjaszewski K. Macromolecules 2006;39:6384.
[40] Coca S, Matyjaszewski K. Macromolecules 1997;30:2808.
[41] Davis KA, Charleux B, Matyjaszewski K. J Polym Sci Part A Polym Chem 2000;38:2274.
[42] Min K, Gao H, Matyjaszewski K. J Am Chem Soc 2005;127:3825.
[43] Davis KA, Matyjaszewski K. Adv Polym Sci 2002;159:1.